ChemComm

Accepted Manuscript

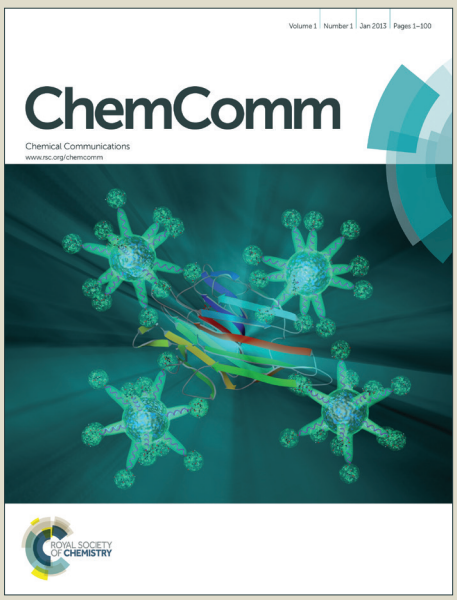

ROYAL SOCIETY OF CHEMISTRY

www.rsc.org/chemcomm

Journal Name

RSCPublishing

COMMUNICATION

Supramolecular hydrogels from cyclic amino acids and their application for the synthesis of Pt and Ir nanocrystals†

Cite this: DOI: 10.1039/x0xx00000x

Received 00th January 2012,
Accepted 00th January 2012

DOI: 10.1039/x0xx00000x

www.rsc.org/

Chuanqing Kang,*[a] Lanlan Wang,[a] Zheng Bian,[a] Haiquan Guo,[a] Xiaoye Ma,[a] Xuepeng Qiu[a] and Lianxun Gao*[a]

New simple hydrogelators containing the structural feature of cyclic amino acids were investigated for water gelation through H-bonds from carboxylic acids and amino groups, which were the first use of a single amino acid as an hydrogelator. The hydrogels was used for the synthesis of Pt and Ir nanoparticles, representing the first time that a supramolecular hydrogel was used for the *in situ* formation of Pt and Ir nanocrystals.

Low-molecular-weight hydrogelators (LMWHs) have received considerable attention for their distinctive properties and potentials in catalytic and biologic applications.[1] Various synthetic molecules have been widely studied for self-assembly into entangled nanofiberous networks for water gelation, of which oligopeptides were mostly reported.[2] A few simple *N*-acylated amino acids, such as *N*-Fmoc protected amino acids and biotin-derived amino acids, are also attractive because of their modular and tunable hydrogelation behaviors, as well as diverse structure and abundant availability.[3] A combination of amino acids with noble metal ion, small molecules, or polymer were also reported in few cases.[4] However, there is no report about the construction of hydrogel based on a single natural or synthetic amino acid so far. Because most LMWHs are serendipitous rather than designed, many efforts are still devoted on developing molecular architectures with tailored functions and capabilities to water gelation.[5] Advances in this area would expand the spectrum of LMWHs and promote the rational design of molecular gelators.

The unique stable and interlocked fibrous networks of gels are suitable matrices for the synthesis of metal nanoparticles (NPs) by the *in situ* reduction of metal salts using chemical, photoinduced, electrochemical, or microwave-assisted methods.[6] Interest to metal NPs-containing gels has grown because of their outstanding physical properties and potential applications.[7] Although some supramolecular gels containing the *in situ* created NPs of Au, Ag, Pd and Pt bave been reported,[8] the metal NPs in gels is not well studied in comparison with those in inorganic or polymeric supporters. Crystallinity received much attention for metal NPs on inorganic supporters but was seldom reported for those in gels. Considering the good catalytic activities of Pt and Ir NPs in the field of green and sustainable chemistry,[9] we have been interested in developing hybrid materials having combined merits of NPs and hydrogels. The formation of nanocrystals in the gel phase was also studied, which was performed in acidic conditions and avoided using external surfactants or stabilizers. In addition, to the best of our knowledge, no case has been reported thus far on IrNPs embedded in gels or the *in situ* creation of NPs with gel matrices.

We recently found that cyclic aminoalcohols based on 1,2,3,4-tetrahydroisoquinoline (THIQ) scaffold can be used for the gelation of organic solvents and the templating synthesis of AuNPs and PtNPs.[10] Then we progressed to THIQ-based cyclic amino acids **1**-**3** (Scheme 1) to investigate the nature of water gelation and its applications for the *in situ* synthesis of Pt and Ir NPs. Thus, we achieved the formation of crystalline Pt and Ir NPs in hydrogels. A supramolecular hydrogel was used for the first time for the *in situ* formation of Pt and Ir nanocrystals. Here, we reported our preliminary results.

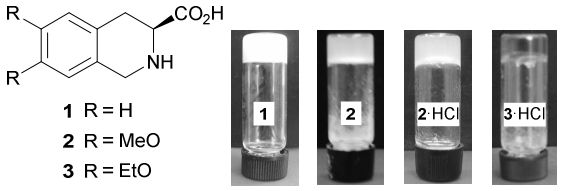

Scheme 1 THIQ-based cyclic amino acids for water gelation

Water gelation with the small and simple molecules **1**-**3** and their HCl salts was determined using the inverse tube method. The simplest compound **1** formed an opaque hydrogel at 2% (wt/wt), but it was easily broken. Precipitates formed from water when a hot solution of **1** was mixed with equal equivalents of HCl. Dimethoxy substituted **2** and **2**·HCl induced water gelation at 1% and 1.5% within 30 min to form translucent and opaque hydrogels, respectively. Compound **3**,

which contains two ethoxy groups, could not gel water, whereas 2% **3**·HCl led to the formation of a transparent hydrogel after standing for 2 h. In addition, the carboxylate sodium salts of **1**, **2** and **3** did not yield water gelation. Salt formation destroyed the potential for H-bonding, which were crucial for water gelation, from carboxylic acids and amino groups. The hydrogels of **2**, **2**·HCl, and **3**·HCl were broken when in contact with small amounts of methanol, suggesting subtle changes of the self-assembly motif in the supramolecular system.

The micromorphologies of the hydrogels were investigated by transmission electron microscopy (TEM). Well-entangled fibrous networks were observed for the hydrogels of **2**, **2**·HCl and **3**·HCl, whereas regular thin films were scattered within the hydrogel of **1** (Fig. 1). According to the gelation tests and these TEM images, it seems that the presence of alkoxy groups at positions 6 and 7 of the THIQ scaffold were crucial factors for determining the formation of fiberous networks as well as stable hydrogels. The alkoxy groups may impose influence on the hydrophilic-hydrophobic balance of the hydrogelators, thus tune the micromorphology of the hydrogels. The poor stability of the hydrogel of **1** was a result of the formation of regular thin films.

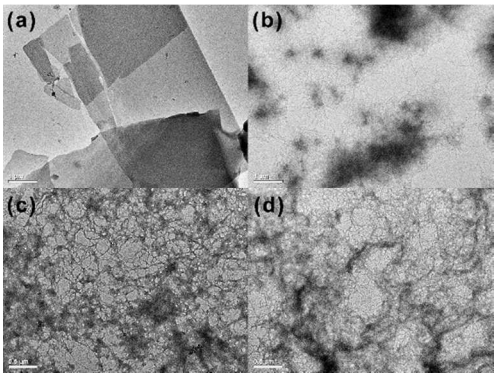

Fig. 1 TEM images of hydrogels of **1** (a), **2** (b), **2**·HCl (c) and **3**·HCl (d). Scale bars: 1 μm for (a) and (b), 0.5 μm for (c) and (d).

The crystal of **2**·HCl suitable for X-ray crystallography analysis was obtained from methanol (Fig. 2). Each crystal cell was composed of four molecules in a form of **2**·HCl·CH_3OH,[11] in which **2** molecules were assembled in the head-to-head arrangement with Cl^- ions and methanol molecules as bridges. Primary H-bonds were formed between amino groups and carboxylic acids from two **2** molecules in opposite position. Additional long H-bond sequences, i.e., N-H···Cl(···H-OCH_3)···H-N and N-H···Cl···H-O(CH_3)···H-O_2C, bridged the adjacent units of **2** and extended the molecular arrangement along the *a* axis of the crystal cell. Next, packing with van der Waals interactions between methoxy groups and aromatic hydrocarbons along the *b* and *c* axes produced a three-dimensional (3D) association in the bilayer stacking pattern, in which the hydrophilic sides were close to each other, and so were the hydrophobic sides (Fig. S1, ESI†).

Insights into the molecular organization in the gel phase were performed with the analysis of powder XRD patterns. In the simulated XRD pattern of the single crystal **2**·HCl (Fig. 3a), the peaks with *d*-spacings of 13.4 Å [plane (002)] and 8.5 Å [plane (011)] were the spaces of the head-to-head stackings and the Cl^- ion-containing H-bonds (Fig. S2, ESI†), respectively. Accordingly, the peak with *d*-spacings of 17.3 Å (though very weak) and 8.1 Å in the powder XRD pattern of the xerogel of **2**·HCl (Fig. 2b) could be assigned to the space of head-to-head stackings with poor orderliness and the space of Cl^- ion-containing H-bonds, respectively. A similar result was shown in the powder XRD pattern of **3**·HCl (Fig. 3c), in which both peaks with *d*-spacings of 17.3 Å and 8.6 Å were much clearer. In the powder XRD pattern of the xerogel of **2** (Fig. 3d), there was a strong peak with *d*-spacings of 19.1 Å attributd to the space of the head-to-head stackings, but no peak related to the Cl^- ions-containing H-bonds. Therefore, both **2**·HCl and **3**·HCl were proposed to be assembled in the gel phase in similar stacking pattern as **2**·HCl in the single crystal. Cl^- ions were expected to form the H-bonds for bridging adjacent molecules to the 1D self-assembly of the gel, as in the single crystal. The replacement of methanol with water disturbed the geometry of the methanol-containing H-bond sequences. The hydrogelators in the gel phase were arranged in a configuration that was not suitable for the 3D self-assembly of the crystal but was beneficial for the 1D self-assembly of entangled fibrous networks.[12] The rupture of the hydrogel in the presence of methanol was probably due to the reorganization of the H-bonds for tendency to bonding with methanol.

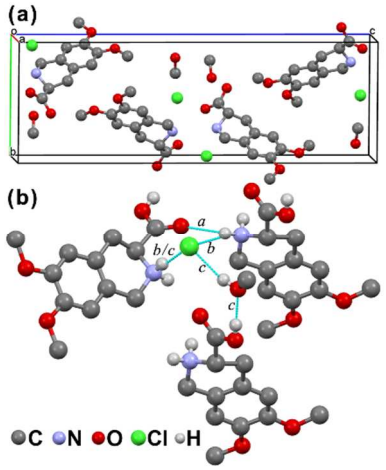

Fig. 2 Single crystal of **2**·HCl·CH3OH: crystal cell (a) and H-bondings (b). Bond *a* was direct H-bonding between carboxylic acid and amino, *b* was N-H···Cl(···H-OCH_3)···H-N and *c* was N-H···Cl···H-O(CH_3)···H-O_2C. Hydrogens on carbons were hidden for clarity.

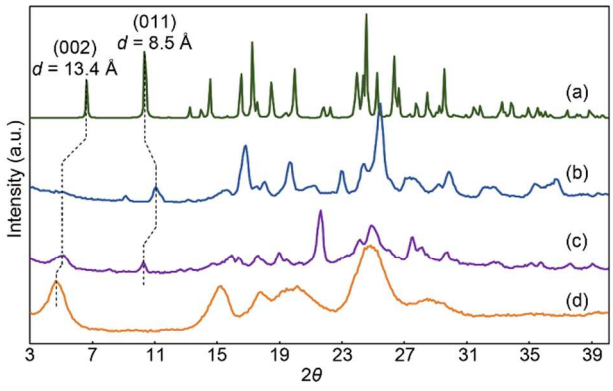

Fig. 3 Simulated powder pattern of the single crystal of **2**·HCl·CH_3OH (a) and powder XRD pattern of the xerogel of **2**·HCl (b), **3**·HCl (c), and **2** (d). The dashed lines indicate the equivalent peaks corresponding to the spaces of the head-to-head stacking and the Cl^- ions-containing H-bonds in the crystal and gel phases.

The hydrogels of **2**·HCl (2% wt/wt) was used as the matrix for the preparation of Pt and Ir NPs. The aqueous solution of H_2PtCl_6 or Na_2IrCl_6 was added to the top of the hydrogels to enable the diffusion of the metal ions into the hydrogel. The upper layers turned nearly colorless, while the hydrogels were colored, suggesting that the metal ions were trapped in the hydrogels. The reduction of Pt and Ir ions to the corresponding NPs was performed using hydrogen and $NaBH_4$ as reductants, respectively. The reduction was completed when the color faded to off-white, which was visually observed. The hydrogel of **3**·HCl was suitable for the synthesis of Ir NPs, but not for the synthesis of Pt NPs. The hydrogel of **3**·HCl containing Pt ions was transited to a solution and eye-visible Pt black was formed during the reduction. The hydrogel of **3**·HCl was sensitive to the increase of HCl concentration from the reduction and the collapse of fiberous network led to the aggregation of PtNPs.

The formation and micromorphology of the metal NPs within the hydrogel matrix were analyzed by TEM and high-resolution TEM (HRTEM). In the TEM images, PtNPs with sizes ranging from 2 nm to 8 nm were observed to be well dispersed (Fig. 4a). Statistical analysis gave an average size of 4.6 nm and a standard deviation of 1.5 nm (Fig. S3a, ESI†), indicating that the fibrous networks of the hydrogel effectively separated the Pt ions and inhibited the accumulation of PtNPs. The HRTEM images showed that the PtNPs had a nearly spherical shape with clear lattice fringes. Most of the PtNPs displayed lattices with a single interplanar spacing of 0.22 nm conforming to the (111) face of the face-centred cubic (*fcc*) Pt, of which some were the aggregates of few smaller nanocrystals (Fig. 4b). Some Pt nanocrystals showed intersecting lattice fringes in two directions with interplanar spacings of 0.22 nm and 0.19 nm indexed to the (111) and (200) faces of *fcc* Pt, respectively (Fig. 4c).[13] The angle between the two indexed lattices was 55 °, which was in agreement with the calculations for the *fcc* Pt, and the diffraction spots indexed to (111) and (200) faces in the corresponding FFT (Fig. S3b, ESI†).

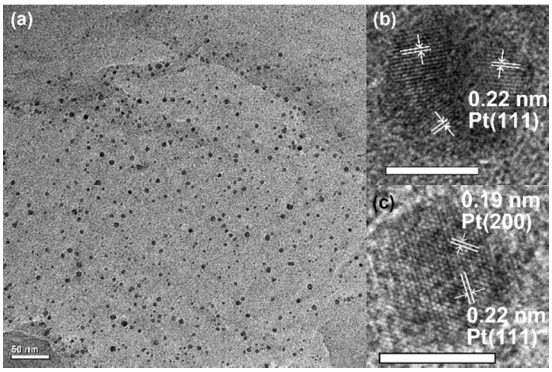

Fig. 4 TEM (a), HRTEM images (b, c) of PtNPs. Scale bars: 50 nm for (a) and 5 nm for (b, c).

The IrNPs in sizes ranging from 3 nm to 10 nm were immersed in the hydrogel matrix (Fig. 5a). Statistical analysis gave an average size of 5.8 nm and a standard deviation of 1.4 nm (Fig. S4a, ESI†). The HRTEM image of the IrNPs showed the formation of nanocrystals with a spherical or irregular polygonal shape, in which lattice fringes had an interplanar spacing of 0.23 nm conforming to the (111) face of the *fcc* Ir (Fig. 5b).[14] Most of the Ir nanocrystals were composed of several smaller nanocrystals (Fig. 5c). Therefore, a polycrystal ring with scattered diffraction spots was observed in the corresponding FFT (Fig. S3b, ESI†). The production of metal NPs suggested the effectiveness of the hydrogel in controlling the synthesis and morphology of Pt and Ir nanocrystals.

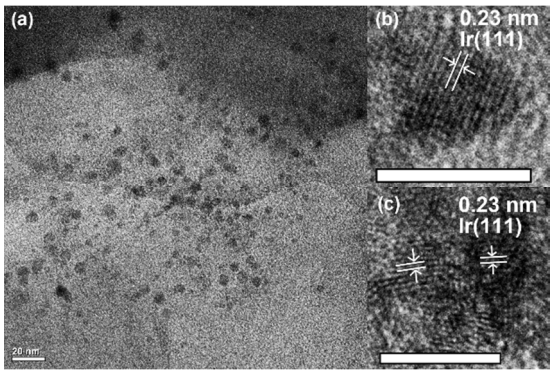

Fig. 5 TEM (a), HRTEM image (b, c) of IrNPs. Scale bars: 20 nm for (a) and 5 nm for (b, c).

The *in situ* synthesized Pt NPs in the hydrogel of **2**·HCl were used as a catalyst for the hydrogenation of nitro substrates **4**s to evaluate the catalytic activity (Fig. 6a). The hydrogenation was one of standard reactions for the evaluation.[15] The Pt NPs in the hydrogel were mixed with aqueous solutions of **4**s followed by addition of $NaBH_4$ as hydrogen source. The reaction mixture was standing at room temperature for 1 h when the reduction was completed according to TLC by comparison with authentic compounds (Fig. S7, ESI†). The success of the catalytic hydrogenation of nitro group to amino group was confirmed by UV-Vis (Fig. 6b). The characteristic absorption peaks of 4-nitroaniline **4a** and 4-nitrophenol **4b** were at 380 nm and 320 nm, respectively, which had completely disappeared after 1 h of reaction time. New absorption peaks at 284 nm and 287 nm were attributed to corresponding amino compounds **5a** and **5b**, respectively. The *in situ* synthesized Ir NPs did not promote the conversion in current conditions.

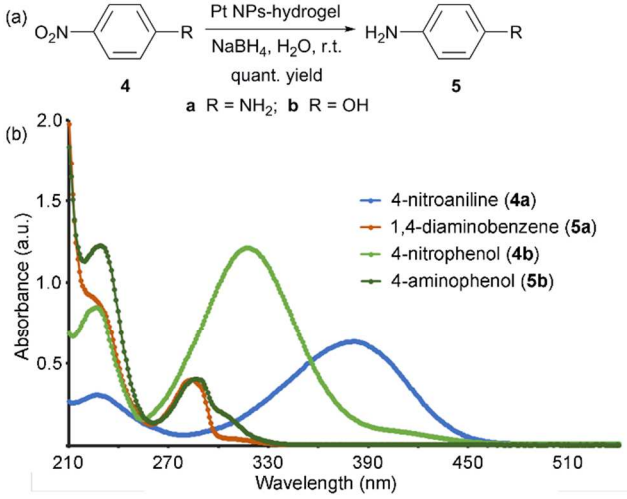

Fig. 6 The Pt NPs-catalyzed reduction of 4-nitroaryls (a) and UV-Vis spectroscopy of 4-nitroaryls and reaction mixtures indicating complete conversion (b).

In summary, we developed new simple hydrogelators derived from 1,2,3,4-tetrahydroisoquinoline with the structural feature of cyclic amino acids. This was the first example using a single amino acid and its HCl salt for water gelation. Long H-bond sequences involving carboxylic acids, amino groups and solvents were discovered to be responsible for the self-

assembly in the crystal and gel phases, the formation of which was determined by the presence of HCl and methanol. The hydrogel of **2**·HCl was effectively used as the matrix for controlling the synthesis, dispersion, and morphology of Pt and Ir nanocrystals with sizes of 4.6 ± 1.5 nm and 5.8 ± 1.4 nm, respectively. No external surfactants or stablilizers were used in the synthesis. According to the HRTEM images, the diffraction lattices in both nanocrystals matched well with the *fcc* geometry. To the best of our knowledge, this is the first report on the use of supramolecular hydrogels as matrices for the synthesis of Pt and Ir nanocrytals. The Pt nanocrystals were successfully used as catalyst for hydrogenation of nitro group. Studies on further catalytic application of NP-hydrogel hybrid materials are in progress.

We would like to thank the Natural Science Foundation of Jilin, China (No. 20130101005JC) and the National Natural Science Foundation of China (No. 21274142) for funding this work.

Notes and references

[a] State Key Laboratory of Polymer Physics and Chemistry, Changchun Institute of Applied Chemistry, Chinese Academy of Sciences, 5625 Renmin Street, Changchun 130022, China. Fax: +86-431-85262926; Tel: +86-431-85262291; E-mail: kangcq@ciac.ac.cn, lxgao@ciac.ac.cn.

† Electronic Supplementary Information (ESI) available: Experimental materials and instruments; water gelation; synthesis and characterization of metal NPs; catalytic reduction with Pt NPs; CIF data of single crystal **2**·HCl·CH_3OH, CCDC: 843101. See DOI: 10.1039/c000000x/

1 (a) T. Tian, J. Chen, R. Niu, *Nanoscale*, 2014, **6**, 3474; (b) A. Döring, W. Birnbaum, D. Kuckling, *Chem. Soc. Rev.*, 2013, **42**, 7391; (c) B. Xu, *Langmuir*, 2009, **25**, 8375; (d) L. A. Estroff, A. D. Hamilton, *Chem. Rev.*, 2004, **104**, 1201.

2 (a) J. Raeburn, A. Z. Cardoso, D. J. Adams, *Chem. Soc. Rev.*, 2013, **42**, 5143; (b) E. A. Appel, J. del Barrio, X. J. Loh, O. A. Scherman, *Chem. Soc. Rev.*, 2012, **41**, 6195; (c) X. Li, Y. Kuang, B. Xu, *Soft Matter*, 2012, **8**, 2801; (d) A. Dasgupta, J. H. Mondal, D. Das, *RSC Advances*, 2013, **3**, 9117; (e) B. Escuder, S. Marti, J. F. Miravet, *Langmuir*, 2005, **21**, 6776.

3 (a) D. Wu, J. Zhou, J. Shi, X. Du, B. Xu, *Chem. Commun.*, 2014, **50**, 1992; (b) S. Roy, A. Banerjee, *Soft Matter*, 2011, 7, 5300; (c) S. Bhuniya, S. M. Park, B. H. Kim, *Org. Lett.*, 2005, **7**, 1741; (d) S. Roy, A. Baral, A. Banerjee, *Chem. Eur. J.*, 2013, **19**, 14950; (e) S. Sutton, N. L. Campbell, A. I. Cooper, M. Kirkland, W. J. Frith, D. J. Adams, *Langmuir*, 2009, **25**, 10285; (f) L. Frkanec, M. Žinić, *Chem. Commun.*, 2010, **46**, 522.

4 (a) F. F. da Silva, F. L. de Menezes, L. L. da Luz, S. Alves, *New J. Chem.*, 2014, **38**, 893; (b) E. Donaldson, J. Cuy, P. Nair, B. Ratner, *Macromol. Symp.*, 2005, **227**, 115; (c) J. Zhang, D.-S. Guo, L.-H. Wang, Z. Wang, Y. Liu, *Soft Matter*, 2011, **7**, 1756; (d) B. Adhikari, J. Nanda, A. Banerjee, *Soft Matter*, 2011, **7**, 8913.

5 (a) J.-B. Guilbaud, A. Saiani, *Chem. Soc. Rev.*, 2011, **40**, 1200; (b) D. D. Díaz, D. Kühbeck, R. J. Koopmans, *Chem. Soc. Rev.*, 2011, **40**, 427; (c) J. H. van Esch, *Langmuir*, 2009, **25**, 8392.

6 (a) N. Sahiner, *Prog. Polym. Sci.*, 2013, **38**, 1329; (b) N. S. Satarkar, D. Biswal, J. Z. Hilt, *Soft Matter*, 2010, **6**, 2364; (c) C. Jiang, W. Qian, *Prog. Chem.*, 2010, **22**, 1626.

7 (a) S. Gai, C. Li, P. Yang, J. Lin, *Chem. Rev.*, 2014, **114**, 2343; (b) D. Das, T. Kar, P. K. Das, *Soft Matter*, 2012, 2348.

8 (a) J. Shen, Y. Chen, J. Huang, J. Chen, C. Zhao, Y. Zheng, T. Yu, Y. Yang, H. Zhang, *Soft Matter*, 2013, **9**, 2017; (b) M. J. Laudenslager, J. D. Schiffman, C. L. Schauer, *Biomacromol.*, 2008, **9**, 2682; (c) A. Zinchenko, Y. Miwa, L. I. Lopatina, V. G. Sergeyev, S. Murata, *ACS Appl. Mater. Interfaces*, 2014, **6**, 3226; (d) B. Corain, K. Jerabek, P. Centomo, P. Canton, *Angew. Chem. Int. Ed.*, 2004, **43**, 959.

9 (a) K. Miyabayashi, H. Nishihara, M. Miyake, *Langmuir*, 2014, **30**, 2936; (b) P. Dai, J. Xie, M. T. Mayer, X. Yang, J. Zhan, D. Wang, *Angew. Chem. Int. Ed.*, 2013, **52**, 11119; (c) A. K. Shil, P. Das, *Green Chem.*, 2013, **15**, 3421; (d) F. Coccia, L. Tonucci, D. Bosco, M. Bressan, N. d'Alessandro, *Green Chem.*, 2012, **14**, 1073; (e) I. S. Park, M. S. Kwon, K. Y. Kang, J. S. Lee, J. Park, *Adv. Synth. Catal.*, 2007, **349**, 2039.

10 (a) Y. Xu, C. Kang, Y. Chen, Z. Bian, X. Qiu, L. Gao, Q. Meng, *Chem. Eur. J.*, 2012, **18**, 16955; (b) C. Kang, Z. Bian, Y. He, F. Han, X. Qiu, L. Gao, *Chem. Commun.*, 2011, **47**, 10746.

11 Crystal data for **2**·HCl·CH_3OH: $C_{13}H_{20}ClNO_5$, M = 305.75, orthorhombic, a = 6.2745(4) Å, b = 9.0192(6) Å, c = 26.8007(17) Å, α = 90.00°, β = 90.00°, γ = 90.00°, V = 1516.68(17) Å^3, T = 296(2) K, space group $P212121$, Z = 4, 8060 reflections measured, 2773 independent reflections (R_{int} = 0.0337). The final R_1 values were 0.0324 ($I > 2\sigma(I)$). The final $wR(F^2)$ values were 0.0742 ($I > 2\sigma(I)$). The final R_1 values were 0.0400 (all data). The final $wR(F^2)$ values were 0.0777 (all data). The goodness of fit on F^2 was 1.028. CCDC number 843101.

12 (a) M. Anne, in *Molecular Gels: Materials with Self-assembled Fibrillar Networks*, ed. R. G. Weiss and P. Terech, Springer, Dordrecht, the Netherlands, 2006, ch. 11, pp. 325-362; (b) A. Shumburo, M. C. Biewer, *Chem. Mater.*, 2002, **14**, 3745; (c) X. Yang, R. Lu, T. Xu, P. Xue, X. Liu, Y. Zhao, *Chem. Commun.*, 2008, 453.

13 (a) C. Zhang, S. Y. Hwang, Z. Peng, *J. Mater. Chem. A*, 2013, **1**, 14402; (b) L. Li, L.-L. Wang, D. D. Johnson, Z. Zhang, S. I. Sanchez, J. H. Kang, R. G. Nuzzo, Q. Wang, A. I. Frenkel, J. Li, J. Ciston, E. A. Stach, J. C. Yang, *J. Am. Chem. Soc.*, 2013, **135**, 13062.

14 (a) C. A. Stowell, B. A. Korgel, *Nano Lett.*, 2005, **5**, 1203; (b) X. Xia, L. Figueroa-Cosme, J. Tao, H. Peng, G. Niu, Y. Zhu, Y. Xia, *J. Am. Chem. Soc.* 2014, **136**, 10878.

15 (a) I. Maity, D. B. Rasale, A. K. Das, *Soft Matter*, 2012, **8**, 5301; (b) L. Zhang, S. Zheng, D. E. Kang, J. Y. Shin, H. Suh, I. Kim, *RSC Advances*, 2013, **3**, 4692.

